Pergamon

Int. J. Heat Mass Transfer. Vol. 40, No. 6, pp. 1303–1311, 1997

0017-9310/97 $17.00+0.00

PII: S0017-9310(96)00202-5

Transport of a passive scalar in a turbulent channel flow

DIMITRIOS V. PAPAVASSILIOU and THOMAS J. HANRATTY†

Department of Chemical Engineering, University of Illinois, Urbana, IL61801, U.S.A.

(*Received* 1 *May* 1996 *and in final form* 31 *May* 1996)

Abstract—Turbulent flow through a channel in which one wall is heated and the other is cooled is considered. Temperature profiles for Prandtl numbers equal to 0.1, 0.7, 1, 3, 10, 100, 500 and 2400 are calculated, by considering the walls to be series of sources and sinks. The spatial variation of eddy conductivity for $Pr = 1$ is interpreted in terms of the time dependency of diffusion from single sources. Support is provided for experimental studies which show that the dimensionless mass transfer coefficient varies as $Sc^{-0.704}$ at large Sc. Copyright © 1996 Elsevier Science Ltd.

1. INTRODUCTION

The basic problem in developing a theory for turbulent transport of mass or heat from a wall is to calculate statistical properties of the scalar concentration field from statistical properties of the velocity field. The classical approach has been to use some form of the Reynolds analogy to relate turbulent transport of a scalar to turbulent transport of momentum (the Reynolds stress). Central concerns are the prediction of the spatial variation of eddy transport coefficients, the effect of molecular Pr and the effect of changes of boundary conditions. The availability of direct numerical simulations (DNS) of turbulent velocity and scalar fluids offers the opportunity to address these issues and to provide a sounder theoretical understanding than is offered by the analogy.

The physics of the transfer of heat or mass evolves in a more natural way when a Lagrangian approach is used [1, 2]. In the Lagrangian framework, the statistical properties of trajectories of heat or mass markers must be known. The main physical challenge is the description and interpretation of the behavior of markers from a single source. Laboratory studies have been hampered because of the difficulty of making measurements in a moving reference frame.

The problem considered in this paper is passive heat transfer in a turbulent flow through a channel in which one wall is heated and the other is cooled. In a Lagrangian analysis the mean temperature field is described as resulting from an infinite number of heat sources at the hot plane and an infinite number of sinks at the cold plane [3].

The behavior of a wall source is determined by following the paths of a large number of scalar markers in a DNS of turbulent flow in a channel. The method of calculating the mean temperature or concentration field from such information has been described by Papavassiliou and Hanratty [4, 5]. In the present paper, results for the transport of heat or mass are presented for Prandtl or Schmidt numbers that span five orders of magnitude (Pr or $Sc = 0.1, 0.7, 1, 3, 10, 100, 500$ and 2400) and describe the heat transfer behavior of liquid metals, gases, liquids and heavy oils. Mean temperature profiles, obtained using the Lagrangian method, are compared with results from an Eulerian DNS with heat transfer. Eddy diffusivity profiles are calculated and the effect of Pr is discussed. Of particular interest are results at large Pr, where the determination of the spatial variation of temperature in laboratory or computer experiments is quite difficult because of the thinness of the scalar boundary layer.

2. BACKGROUND

2.1. *Turbulent transport of heat or mass in a Eulerian frame-work*

In a Eulerian description of turbulent transport, the temperature‡, T, is decomposed as $T = \bar{T} + t'$. The temperature can be made dimensionless by using the friction temperature, $T^* = q_w/\rho C_p u^*$. The heat flux at the wall is defined in terms of the thermal conductivity k as

$$q_w = -k\left(\frac{d\bar{T}}{dy}\right)_w. \quad (1)$$

The dimensionless temperature in wall units, T^+, is then defined as

† Author to whom correspondence should be addressed.

‡ The scalar quantity used in this paper is the temperature and the dimensionless number is the Prandtl number, Pr. The results can be applied directly to the case of turbulent mass transfer by replacing temperature with concentration and Prandtl number with Schmidt number, Sc.

NOMENCLATURE

A constant in the power law relation for the heat transfer coefficient
b coefficient in the eddy conductivity relation, equation (15)
C_p specific heat at constant pressure
D molecular diffusivity
E_c eddy conductivity
E_v eddy viscosity
h half channel height
K heat transfer coefficient
k thermal conductivity
l mixing length
m exponent in the eddy conductivity, equation(7)
n exponent that describes the variation of E_c with the distance from the wall
P_1 conditional probability for a marker to be at a certain location, given that it was released from the wall
P_2 marginal probability for a marker to be at a distance y from the wall (see equation (10))
Pr Prandtl number v/α
Pr_t turbulent Prandtl number $= E_y/E_c$
q heat flux
q_w heat flux at the channel wall
R^L Lagrangian correlation coefficient
Re Reynolds number $= U_c h/v$
Sc Schmidt number $= v/D$
T temperature
T_c temperature at the center of the channel
T_w temperature at the wall of the channel
T^* friction temperature
$\bar{T}$ mean temperature
t time
t_o time instant of marker release
t' temperature fluctuation
u^* friction velocity $= (\tau w/\rho)^{1/2}$
$\mathbf{U}$ Eulerian velocity vector
$\bar{U}$ mean velocity
u', v', w' fluctuating velocity components in the x-, y-, z-directions
x, y, z streamwise, normal and spanwise coordinates
X displacement of a marker from the source in the x-direction
$\mathbf{X}$ position vector of a marker
$\tilde{x}_o$ initial position of a marker
$\overline{y^2}$ mean squared dispersion in the normal direction
w weight function, defined in equation (13)
$\overline{z^2}$ mean squared dispersion in the spanwise direction.

Greek symbols

α thermal diffusivity
λ_x, λ_z periodicity lengths of the flow in the streamwise and spanwise directions
v kinematic viscosity
π trigonometric pi
ρ fluid density
σ standard deviation of a probability density function
τ_w shear stress at the wall.

Superscripts and subscripts

$\overline{(\,)}$ ensemble average
$(\,)'$ fluctuating quantity
$(\,)^L$ Lagrangian variable
$(\,)^+$ value made dimensionless with the wall parameters
$(\,)^*$ friction value
$(\,)_c$ value at the center of the channel
$(\,)_o$ value at the instant of marker release
$(\,)_t$ contribution from turbulence
$(\,)_w$ value at the wall.

$$T^+ = \frac{T}{T^*} = -\frac{T\rho C_p u^*}{\left(k\frac{d\bar{T}}{dy}\right)_w} = -Pr\frac{T}{\left(\frac{d\bar{T}}{dy^+}\right)_w} \quad (2)$$

where y^+ is the distance from the wall in viscous wall units ($y^+ = yu^*/v$). A dimensionless eddy conductivity can be defined as

$$E_c^+ = -\frac{\overline{t'^+ v'^+}}{\left(\frac{d\overline{T}^+}{dy^+}\right)}. \quad (3)$$

In a fully developed state the heat flux is constant through the channel and a dimensionless heat transfer coefficient, K^+, can be defined as

$$K^+ = \frac{K}{\rho C_p u^*} \quad (4)$$

with K given by the relation

$$q_w = K(\bar{T}_c - \bar{T}_w). \quad (5)$$

Equations (1), (5) and the definitions (4) and (2) can be used to derive the following relation

$$K^+ = \frac{1}{Pr}\left[\frac{d\left(\frac{\bar{T}}{\bar{T}_c - \bar{T}_w}\right)}{dy^+}\right]_w. \quad (6)$$

At high Pr, the temperature boundary layer is very

thin and the velocity field in it can be described using a Taylor series expansion in terms of y^+. The analogy between momentum and heat or mass transfer gives the eddy conductivity as $E_c^+ \sim y^{+n}$, where n is an integer greater than or equal to three, and a power law relation for K^+

$$K^+ = APr^m. \tag{7}$$

Arguments have been presented in the literature for $m = -2/3$ or $m = -3/4$, depending on whether the eddy conductivity E_c^+ is proportional to y^{+3} or y^{+4}. Shaw and Hanratty [6] obtained very accurate measurements for turbulent mass transfer to the wall of a pipe at Sc between 693 and 39 300 with electrochemical techniques. Their conclusion is that $K^+ = 0.889Sc^{-0.704}$. Campbell and Hanratty [7] and Vassiliadou and Hanratty [8] argued that different parts of the frequency spectrum of the velocity component normal to the wall, v', control transfer at different Sc. They used both numerical and experimental results to show that, as Sc increases, the frequencies of v' fluctuations that contribute to turbulent transport from the wall decrease.

2.2. *Lagrangian turbulent transport*

Einstein [9] developed a relation that describes the dispersion of fluid particles in a non-turbulent field in terms of the mean-squared displacement from the source in the x-direction:

$$\frac{d\overline{X^2}}{dt} = 2D. \tag{8}$$

Taylor [10] developed a similar relation for dispersion of particles from a point source in homogeneous, isotropic turbulence:

$$\frac{d\overline{X^2}}{dt} = 2\overline{u^2}\int_0^t R^L(\tau)\,d\tau \tag{9}$$

where $\overline{u^2}$ is the mean-square of the x-component of the velocity of fluid particles. An important implication of equation (9) is that the history of the particle motion affects the rate of dispersion through R^L.

Dispersion of heat or mass markers introduces an additional complication, since the markers can move off a fluid particle as a result of molecular diffusion. Saffman [11] developed a relation for dispersion in this case by defining a material autocorrelation function, which differs from the Lagrangian correlation in that it correlates fluid velocity components along the trajectories of markers instead of fluid particles.

Hanratty [3] used Taylor's theory to describe the transfer of heat in turbulent channel flow. An infinite number of line sources of heat along one wall was used to describe the hot plane and an infinite number of line sinks of heat along the other wall described the behavior of the cold plane. The variation of the eddy conductivity with the distance from the wall could be associated with the time dependency of turbulent diffusion. Temperature gradients close to the wall were found to result from thermal markers that had been in the field for small periods of time. A difficulty with this analysis is that a homogeneous isotropic velocity field with no mean velocity gradients was assumed. Poreh and Cermak [12], Raupach and Legg [13], Parantheon *et al.* [14] and Incropera *et al.* [15] have carried out experimental studies of wall sources. However, none of these give the space–time behavior of an instantaneous source.

3. NUMERICAL PROCEDURE

The velocity field of a Newtonian and incompressible fluid is calculated using a DNS of fully developed turbulent flow in a channel developed by McLaughlin [16, 17]. The Reynolds number, Re, defined with the centerline mean velocity and half-height of the channel, h, is 2660. The simulation is done on a $128 \times 65 \times 128$ grid in x, y, z axes. The streamwise direction is x, the spanwise is z and the direction perpendicular to the walls of the channel is y. The dimensions of the computational box are $4\pi h \times 2h \times 2\pi h$, with $h = 150$ in wall units. The flow is assumed to be periodic in the streamwise and spanwise directions with periodicity lengths λ_x and λ_z equal to the dimensions of the box in the respective directions. All variables are made dimensionless with wall parameters.

The heat transfer equation in the Eulerian framework is solved for the case of passive heat transfer through this channel using the algorithm proposed by Circelli and McLaughlin [18]. Results for $Pr = 1$ have been presented by Lyons *et al.* [17]. Brooke [19] carried out simulations for $Pr = 0.05$, 0.1, 0.3, 0.6, 3 and 10. In these calculations the temperature at the bottom wall was kept at T_w and the temperature of the top wall at $-T_w$. The heat flux does not vary with y, when a stationary state is reached. The calculation for $Pr = 10$ required the use of a finer grid and special precautions in selecting the time step.

The trajectories of heat or mass markers released from a wall are calculated in the hydrodynamic field created by the DNS. The particle tracking method developed by Kontomaris *et al.* [20] is used. The basic assumption is that a heat marker at each time has the velocity of the fluid particle that carries it. The equation of particle motion is integrated using an Adams–Bashforth scheme (explicit, second-order accurate). Each marker moves due to two effects, the convective effect and the molecular effect. The convective part of the motion is calculated from the fluid velocity at the particle position. The effect of molecular diffusion is simulated by imposing a three-dimensional random walk on the particle motion; it is added on the convective part of the motion after each time step, Δt, and takes values from a Gaussian distribution with zero mean and standard deviation $\sigma = \sqrt{2\Delta t/Pr}$, in wall units [5, 21]. The description of the diffusion process by a random walk of a large

number of particles in a 3-D space has been reviewed in detail by Chandrasekhar [22]. By using a mixed Lagrangian–Chebyshev interpolation scheme to calculate the velocity vector between grid points, it is possible to track the heat or mass markers.

Two sets of tracking experiments were performed. In the first set, Prandtl numbers of 0.1, 1, 10 and 100 were studied with 16129 markers released instantaneously for each Pr in the same velocity field. The initial position of the markers was on a uniform 127×127 grid that covered the bottom wall of the channel. The velocities and positions of these markers were stored every wall time unit for statistical post-processing. In the second set, a different velocity field was used to start the calculations. The Prandtl numbers for the markers were 0.7, 1, 3, 500 and 2400. Each set of computer experiments was carried out on one processor of a CONVEX C3880 supercomputer, up to 2750 wall time units. About 27 CPU hours for 500 time iterations were needed. The time step for both the hydrodynamics and the tracking algorithm was $\Delta t = 0.25$.

The Lagrangian approach allows the study of cases with Pr much larger than is possible in a Eulerian DNS, where extremely find grids and very small time steps are necessary to resolve the steep temperature gradients close to the wall for $Pr > 10$.

4. LAGRANGIAN METHOD

The building block for the Lagrangian formulation is the probability function, $P_1(x-x_o, y, t-t_o|t_o = 0, x_o = 0)$, which is the joint conditional probability for a marker to be at a location (x, y) in the flow at time t, given that the marker was released from the wall at $x_o = 0$ at time $t_o = 0$. The physical interpretation of P_1 is that it represents the evolution in time of a cloud of markers released instantaneously from a line source at the wall. For each experiment, the trajectories of 16129 markers are used as an ensemble to obtain P_1. Since the flow field is homogeneous in the x- and z-directions, there is no statistical dependence on the initial location of the markers.

Probability P_1 can be used to extract information about the behavior of a continuous line source at x_o by integrating over time. The behavior of a heated plane is described with a series of continuous line sources covering the plane. Therefore, the mean temperature profile in a channel, where heat is added to the fluid from the bottom wall at a constant rate and removed from the top at the same rate (iso-flux conditions), can be synthesized from P_1 [5]. The contribution of the bottom wall can be obtained by integrating P_1 over time and over the streamwise direction.

$$P_2(y|t_o, x_o) = \int_{x_o}^{\infty}\int_{t_o}^{\infty} P_1(x-x_o, y, t-t_o|t_o, x_o)\,\mathrm{d}t\,\mathrm{d}x. \tag{10}$$

Distribution P_2 can be interpreted physically as the mean temperature profile resulting from a heated infinite plane. In the case of a channel, the contribution of the cold wall is assumed to be independent of that of the hot wall. The mean temperature profile, $\bar{T}(y)$, can therefore be defined from P_2 as

$$\bar{T}(y) = P_2(y) - P_2(-y) \tag{11}$$

where $y = 0$ corresponds to the center of the channel.

The Eulerian simulations used $T_w = \text{const.}$ as the boundary condition for the mean temperature at the wall. In order to compare the Lagrangian results to the isothermal wall data, a weight function, $w(t)$, is introduced so that the number of markers at the wall stays constant throughout the time integration. Equation (10) is modified as follows:

$$P_2(y|t_o, x_o) = \int_{x_o}^{\infty}\int_{t_o}^{\infty} P_1(x, y, t|t_o, x_o)w(t)\,\mathrm{d}t\,\mathrm{d}x \tag{12}$$

where $w(t)$ is given by

$$w(t) = \frac{T_w - T(y = -h, t)}{T_w} \tag{13}$$

and $T(y = -h, t)$ is the temperature at the wall as time proceeds.

Probability P_2 was calculated for each Pr using a non-uniform bin width, since Chebyshev collocation points were used to increase the resolution closer to the wall. A total of 128 bins spanning the width of the channel were used for $Pr < 10$ and 256 bins for $Pr \geqslant 10$.

The method for obtaining the mean temperature was tested for the case of laminar flow. The exact solution for heat transfer through a semi-infinite slab is given by Bird *et al.* [23]. For $Pr \geqslant 10$, excellent agreement was obtained when the time step for the molecular motion was sufficiently small. These studies demonstrated the adequacy of a sample size of 16129 markers and the need to use a smaller time step for the initial period of the calculations when molecular motion dominates turbulence in transferring heat. The period for which molecular motion is controlling can be obtained by comparing the Lagrangian results to Einstein's relation for molecular diffusion (equation(8)). Values of 15, 40, 55 and 115 viscous time units are estimates for $Pr = 10$, 100, 500 and 2400. In order to obtain more accurate results for these Pr, an exact probability density function for a single point source in laminar flow was used for P_2 during the initial period of the simulation

$$P_2 = \frac{1}{2\sqrt{\pi t/Pr}}\exp\left(-\frac{y^2}{4t/Pr}\right). \tag{14}$$

When a stationary state is reached, the markers from a single source are expected to be uniformly distributed over the width of the channel because the walls of

the channel confine the extent of the field in the y-direction. Therefore, the contribution of a single line source in equation (12) must be considered until the mean displacement of the markers asymptotically reaches a value h or the variance of the displacement reaches the value for a uniform distribution over a region of size $2h$, which is the normal dimension of the channel. At high Pr, however, the mean temperature profile is almost flat in the center region of the channel so it is not necessary to carry out the simulation to times where a uniform marker distribution is achieved. Another criterion for the convergence of the mean temperature profile can be obtained by examining the variation of K^+, calculated from equation (4), with time. The values of K^+ change very little after $t^+ = 2000$.

The two runs at $Pr = 1$ help to assess the statistical variations of the results. A different velocity field was used to initiate the simulations. There is less than 1% difference in both the mean displacement and the root mean squared displacement of the markers through $t^+ = 2500$. These differences are reflected in variations of the $\bar{T}$ profile for $Pr = 1$. Ideally, a large number of computer experiments for each Pr should be conducted; an average of these results would give a more precise determination of $\bar{T}$.

5. RESULTS

5.1. *Mean temperature profiles and transport parameters*

Figure 1 presents the calculated fully developed mean temperature profile across the channel using the Lagrangian method (equations (11), (12)) for all Pr considered. The Eulerian results for $Pr = 0.1$, 1 and 10 are also presented for comparison. Mean temperature profiles in viscous wall units for $Pr = 0.1$, 0.7, 1, 3 and 10 are presented in Fig. 2, along with the mean velocity profile in semi-log coordinates. An extensive well defined logarithmic layer is not evident, especially for $Pr \leqslant 1$.

The spatial variation of the eddy viscosity in the limit of $y^+ \to 0$ can be obtained by using a Taylor

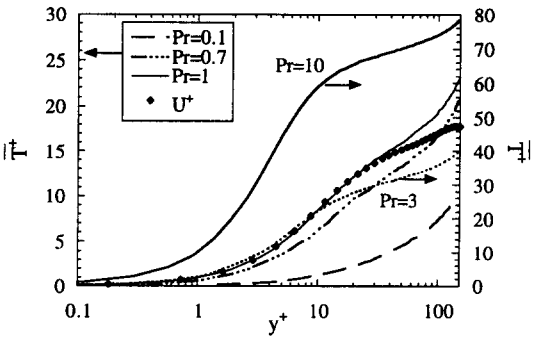

Fig. 2. Mean temperature and mean velocity profiles in viscous wall units.

series description of the velocity field, $E_v^+ = 0.000792y^{+3}$. The constant came from the DNS (Lyons *et al.* [16]). The following power law relation is used for the eddy conductivity at $y^+ \to 0$:

$$E_c^+ = b(Pr)y^{+n} \tag{15}$$

where the coefficient b may be a function of Pr. For $Pr = 1$, the DNS shows $n = 3$ and $b = 0.000775$.

The heat balance equation for the temperature field under consideration is

$$-\frac{\partial \overline{T^+}}{\partial y^+}(Pr^{-1} + E_c^+) = 1. \tag{16}$$

This can be integrated to give

$$\overline{T_w} - \overline{T^+} = \int_0^{y^+} \frac{dy^+}{Pr^{-1} + by^{+n}} \tag{17}$$

if equation (15) is used to define E_c^+. The mean temperature profile close to the wall in viscous wall units is shown in Fig. 3 for $Pr = 100$, 500 and 2400. The points represent values of $\overline{T_w} - \overline{T^+}$. The asymptotic values reached at large y^+ are indicated by thick lines. The solid curves show temperature profiles calculated from equation (17) using the relation $E_c^+ = b(Pr)y^{+3.38}$. The exponential value of 3.38 was suggested by Shaw and Hanratty [6] based on their

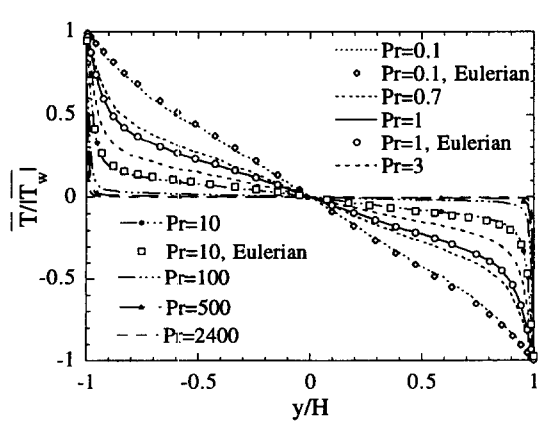

Fig. 1. Mean temperature profiles.

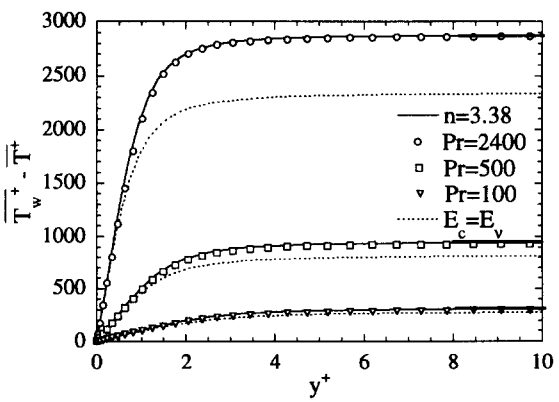

Fig. 3. Mean temperature profiles for the high Pr cases close to the wall.

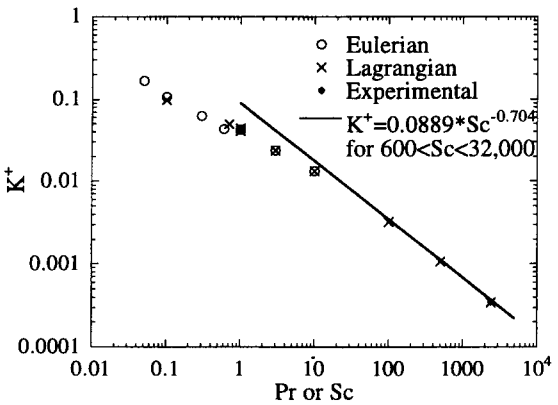

Fig. 4. Heat transfer coefficient as a function of Pr or Sc.

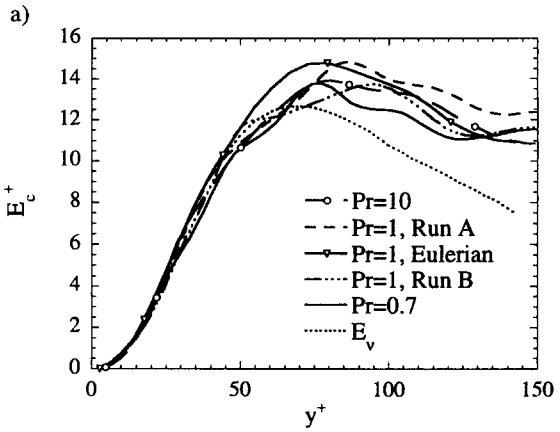

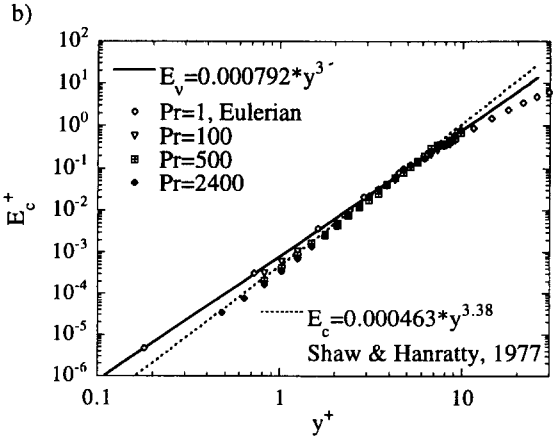

Fig. 5. (a) Eddy conductivity and eddy viscosity profiles; (b) eddy conductivity close to the wall of the channel for high Pr or Sc numbers.

measurements. They also suggested a constant value for $b = 0.000463$. The data here are represented with $b = 0.000502$ for $Pr = 100$, $b = 0.000490$ for $Pr = 500$ and $b = 0.000494$ for $Pr = 2400$. Temperature profiles calculated by assuming $E_c = E_v = 0.000792y^3$ are indicated by the dotted curves in Fig. 3.

The transfer coefficient, K^+, is presented as a function of Pr in Fig. 4. The Eulerian calculations are also given. The dark point at $Pr = 2400$ has been obtained experimentally for the case of mass transfer in a pipe in three separate studies [24–26]. The Lagrangian value closely agrees with the experiments. Note that the two runs for $Pr = 1$ and the Eulerian simulation show almost exact agreement. The straight line represents the relation by Shaw and Hanratty [6]. The calculations for higher Pr appear to confirm this relation.

Profiles of E_c^+ for low Pr and the E_v profile for the transfer of momentum, are shown in Fig. 5(a). The Eulerian results are calculated by using equation (3) and the Lagrangian results by using

$$E_c^+ = \frac{1}{\dfrac{\mathrm{d}\overline{T^+}}{\mathrm{d}y^+}} - \frac{1}{Pr}. \tag{18}$$

The turbulent Prandtl number, is close to unity in the region near the wall. Toward the center of the channel the eddy viscosity line drops below the eddy conductivity lines. Using Eulerian calculations for $Pr = 1$, Pr_t is found to be approximately 0.7 in the center region of the channel.

The eddy conductivities, obtained with the Lagrangian calculation at high Pr, are shown in Fig. 5(b). Logarithmic coordinates are used to expand the region very close to the wall. The eddy conductivity for $Pr = 1$ varies with the cube of the distance from the wall, as does the eddy viscosity, but the eddy conductivities for $Pr = 100$, 500 and 2400 appear to follow power law relations with different exponentials. The dashed line in Fig. 5(b) shows the relation that was suggested from the experiments of Shaw and Hanratty [6] for $700 < Sc < 37\,200$. The results presented here for $Pr = 100$, 500 and 2400 may not be adequate, statistically, for the development of a firm relation. However, they agree approximately with the Shaw relation and strongly suggest that the value of the exponent in equation (15) is not three.

5.2. *Lagrangian interpretation*

The mean temperature gradient at a fixed distance away from the wall results primarily from markers that were released in the flow during a particular time interval. Markers that are in the flow field for longer times affect the regions near the center of the channel; markers that were released in the flow more recently affect regions closer to the wall.

A measure of the time period that contributes to the development of the mean temperatures can be obtained from Fig. 6. It shows the shape of the mean temperature profile at different distances from the wall for $Pr = 1$, calculated from equations (11) and (12). The time coordinate is the upper limit of the integral representing P_2

$$P_2(y|t_o, x_o) = \int_{x_o}^{\infty}\int_{t_o}^{t} P_1(x, y, t|t_o, x_o)w(t)\,\mathrm{d}t\,\mathrm{d}x. \tag{19}$$

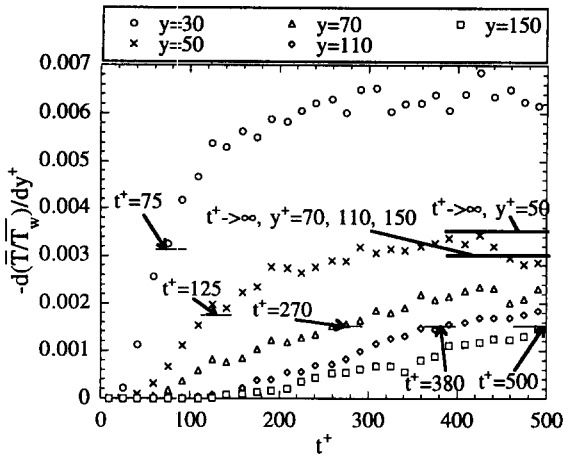

Fig. 6. Contribution to the development of the mean temperature profile at different distances from the wall of the channel ($Pr = 1$).

In Fig. 6 the times at which 50% of the final temperature gradient is captured are marked. For example, at $y^+ = 30$ the temperature gradient is established by markers that were released over the time interval $t^+ = 10$–250. The median is at $t^+ = 75$. Contributions to the temperature gradient at $y^+ = 150$ are made only by markers that have been in the field for $t^+ > 150$. This graph illustrates how the time history of the markers plays an important role in determining the spatial variation of $d\overline{T}^+/dy^+$ (or of E_c^+).

This idea is explored further in Figs. 7 and 8. A relation similar to the one developed by Einstein (equation (8)) can be used to characterize the rate of dispersion of the markers due to turbulence. The rate of dispersion may be considered to be the sum of the contributions from molecular diffusion and turbulent mixing. Thus

$$\frac{d\overline{z^2}}{dt} = \left(\frac{d\overline{z^2}}{dt}\right)_t + 2D \qquad \frac{d\overline{y^2}}{dt} = \left(\frac{d\overline{y^2}}{dt}\right)_t + 2D \tag{20}$$

and

$$\left(\frac{d\overline{z^2}}{dt}\right)_t \sim 2E_c. \tag{21}$$

Terms $(d\overline{z^2}/dt)_t$ and $(d\overline{y^2}/dt)_t$ are plotted in Fig. 7(a) and (b). Increases in $(d\overline{z^2}/dt)_t$ at small times are associated with increases in the turbulent intensity seen by the particles and with the time-dependency of turbulent dispersion. At large times, $(d\overline{z^2}/dt)_t$ reaches an approximately constant value which is the same for $Pr = 1$, 10 and 100. Dispersion in the y-direction, $(d\overline{y^2}/dt)_t$, is seen to decrease with time at large times (see Fig. 7(b), because of nonhomogeneities of the turbulence and because $\overline{y^2}$ has an upper limit due to the confinement of the channel walls.

Using Fig. 7(a), it is possible to estimate the turbulence dispersion rate at the median lifetime of markers contributing to E_c^+ at a given y^+ (indicated in Fig. 6). For all of these median times the number of markers at the top wall was too small for confinement to have an effect. Equation (21) then provides estimates of the eddy conductivity at a given y^+, if t in Fig. 7 is taken as the median indicated in Fig. 6. Figure 8 compares the results of this calculation with values of E_c obtained with the Eulerian and Lagrangian simulations at $Pr = 1$. The agreement of this Lag-

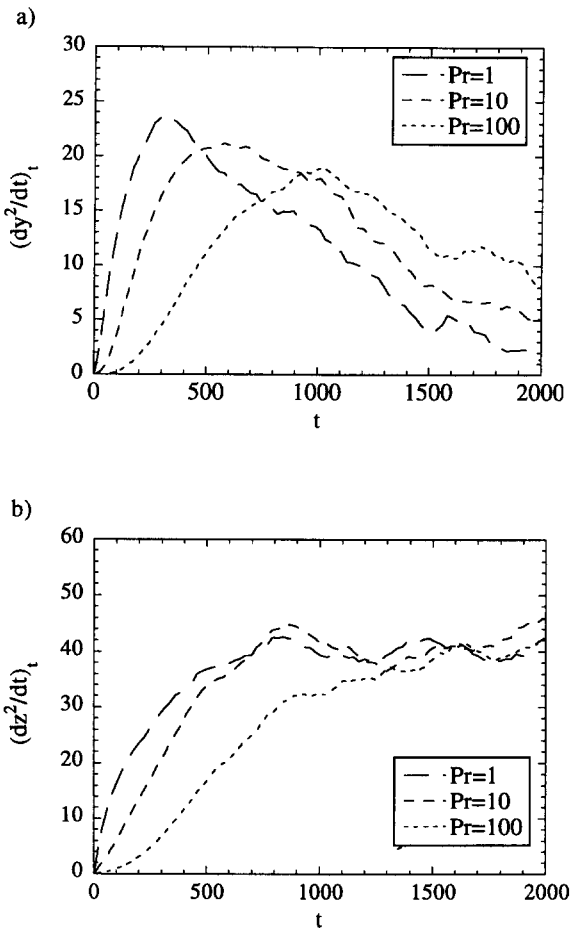

Fig. 7. Dispersion rate. (a) Normal direction; (b) spanwise direction.

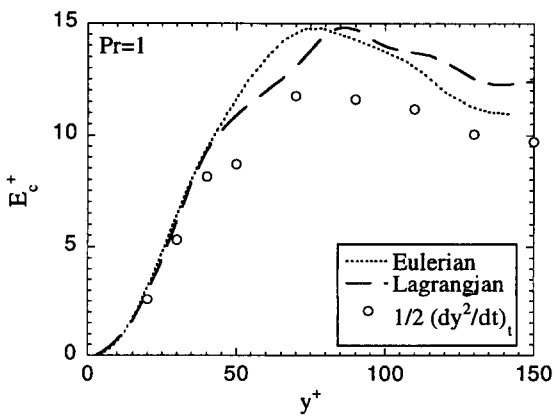

Fig. 8. Lagrangian reconstruction of the eddy conductivity profile.

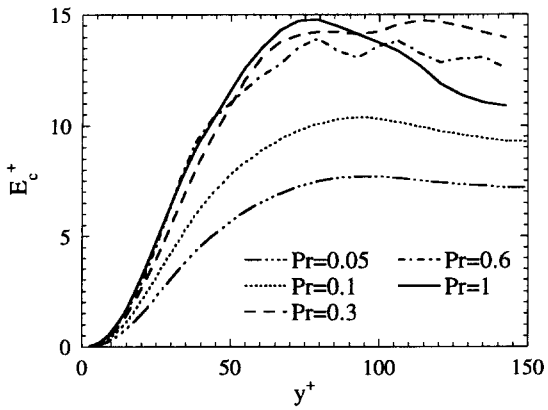

Fig. 9. Eddy conductivity profile for relatively low *Pr*.

rangian reconstruction with the simulation values is as close as could be expected. Better agreement would be obtained if markers in the viscous sublayer (where turbulent transport is zero) were ignored in constructing Fig. 8.

Figure 9 compares eddy conductivies for $Pr = 1$ and for low *Pr*, obtained with the DNS. A large decrease of E_c, with decreasing *Pr*, is noted. One can interpret this effect in terms of mixing-length concepts whereby thermal markers are transported by large scale eddies over a distance, l, characterizing the extent of the coherent motion. Mixing with the surrounding fluid occurs by small scale turbulence, so that the scalar markers are lost at the end of an excursion. The decrease in E_c occurs because large molecular conductivities can cause markers to escape from an eddy and, thereby, decrease its effectiveness in transporting heat (see Kontomaris and Hanratty [21] for a more precise treatment of this effect).

In view of the above, it is of interest that eddy conductivities are observed to decrease from the value for $Pr = 1$ in the viscous sublayer at large *Pr*. In this region the extent of convective motions and the range of spatial scales are very small. It could be pictured as a complicated unsteady viscous flow. A heat marker with zero conductivity would closely follow temporal oscillations since mixing by small scale motions might not be important. Consequently, a finite conductivity is needed in order for mixing to occur during an oscillation. This interpretation is consistent with that given by Campbell and Hanratty [7] and by Hanratty and Vassiliadou [8] in that one would expect high frequency oscillations to be less effective in transporting heat. Consequently, fluctuations in mass transfer rate at the wall would decrease with increasing *Sc* (as demonstrated by Shaw and Hanratty [6]).

6. CONCLUSIONS

The Eulerian description of temperature fields in a turbulent flow requires the specification of the turbulent diffusivity, which can be a function of space, *Pr* number and boundary conditions. A physical understanding of these functionalities is not, at present, available. An alternate approach is to use a Lagrangian framework, whereby the temperature field is pictured as resulting from a distribution of infinitesimal sources (or sinks) at the wall. The theoretical problem, then, is to provide a statistical description of one of these sources. For the case of a fully-developed velocity field the dispersion of heat markers from a source at the wall is a function of the time the markers have been in the field and of *Pr*.

The methodology of using information on the behavior of an instantaneous point source to analyze a variety of heat transfer problems has already been illustrated by the authors [5]. This paper uses this approach to examine the effects of Prandtl number. The simple problem of a fully developed temperature field is examined for turbulent flow in a channel. The top and the bottom walls are kept at constant, but different, temperatures. Of particular interest is the demonstration that it is possible to use these techniques at arbitrarily large *Pr*.

An attempt is made to relate the Lagrangian and Eulerian analyses by considering calculated turbulent diffusivities at $y^+ \geqslant 20$ for $Pr = 1$. The main point of interest in this comparison is that the spatial variation of E_c^+ observed in Eulerian analyses might not be entirely due to spatial variations of the turbulence. Much of it could result from a time-dependency of turbulent diffusion similar to what was described by Taylor in his analysis of point source diffusion in a turbulent field.

For $Pr \leqslant 10$, the turbulent Prandtl number is found to be approximately equal to unity if $y^+ < 40$. However, for $Pr = 100$, 500 and 2400 the turbulent Prandtl number is found to be less than unity. The approach usually taken is to represent the spatial variation of turbulent diffusivity as varying with y^{+3} for $y^+ \to 0$. As indicated above, this is supported for $Pr \leqslant 10$. This assumption predicts that $K^+ \sim Pr^{-2/3}$ at large *Pr*. However, experiments by Shaw and Hanratty for $700 < Sc < 37\,200$ give $K^+ \sim Sc^{-0.704}$. These results have not been used by other investigators because there is some concern as to whether the differences shown in this study reflect experimental error. Therefore, it is of considerable interest that the present analysis is in good agreement with the measurements of Shaw and Hanratty; they do not give a y^3 dependency of the turbulent diffusivity at large *Pr*.

Acknowledgements—This work is being supported by the National Science Foundation through grant CTS-95-03000. We also acknowledge the support and facilities of the National Center for Supercomputing Applications at the University of Illinois in Urbana, Illinois.

REFERENCES

1. Monin, A. S., and Yaglom, A. M., *Statistical Fluid Mechanics: Mechanics of Turbulence*. Vol. 1. MIT Press, Cambridge, MA, 1971.
2. Hunt, J. C. R., Turbulent diffusion from sources in com-

plex flows. *Annual Review of Fluid Mechanics*, 1985, **17,** 447–485.
3. Hanratty, T. J., Heat transfer through a homogeneous isotropic turbulent field. *A.I.Ch.E. Journal*, 1956, **2,** 42–45.
4. Papavassiliou, D. V. and Hanratty, T. J., The use of Lagrangian methods to describe turbulent transport of heat from a wall. *Industrial Engineering Chemical Research*, 1995, **34,** 3359–3367.
5. Papavassiliou, D. V. and Hanratty, T. J., Synthesis of temperature fields in terms of the behavior of instantaneous wall sources. *Proceedings of the Tenth Symposium on Turbulent Shear Flows*, Vol. 3. University Park, PA, 1995.
6. Shaw, D. A. and Hanratty, T. J., Turbulent mass transfer to a wall for large Schmidt numbers *A.I.Ch.E. Journal*, 1977, **23,** 28–37.
7. Campbell, J. A., and Hanratty, T. J., Mechanism of turbulent mass transfer at a solid boundary. *A.I.Ch.E. Journal*, 1983, **29,** 221.
8. Hanratty, T. J., and Vassiliadou, E., Turbulent transfer to a wall at large Schmidt numbers. In *Transport phenomena in turbulent flows. Theory, Experiment and Numerical Simulation*, eds M. Hirata and N. Kasagi. Hemisphere, New York, 1988, pp. 255–274.
9. Einstein, A., *Annals Physika*, 1905, **17,** 549.
10. Taylor, G. I., Diffusion by continuous movements. *Proceedings of the London Mathematics Society*, 1921, **24A,** 196–212.
11. Saffman, P. G., On the effect of the molecular diffusivity in turbulent diffusion. *Journal of Fluid Mechanics*, 1960, **8,** 273–283.
12. Poreh, M. and Cermak, J. E., Study of diffusion from a line source in a turbulent boundary layer. *International Journal of Heat and Mass Transfer*, 1964, **7,** 1083–1095.
13. Raupach, M. R. and Legg, B. J., Turbulent dispersion from an elevated line source: measurments of wind-concentration meoments and budgets. *Journal of Fluid Mechanics*, 1983, **136,** 111–137.
14. Paranthoen, P., Fouari, A., Dupont, A. and Lecordier, J. C., Dispersion measurements in turbulent flows (boundary layer and plane jet). *International Journal of Heat and Mass Transfer*, 1988, **31,** 153–165.
15. Incropera, F. P., Kerby, J. S., Moffatt, D. F. and Ramadhyani, S., Convection heat transfer from discrete heat sources in a rectangular channel. *International Journal of Heat and Mass Transfer*, 1986, **29,** 1051–1058.
16. Lyons, S. L., Hanratty, T. J. and McLaughlin, J. B., Large-scale computer simulation of fully developed turbulent channel flow with heat transfer. *Numerical Methods with Fluids*, 1991, **13,** 999–1028.
17. Lyons, S. L., Hanratty, T. J. and McLaughlin, J. B., Direct numerical simulation of passive heat transfer in a turbulent channel flow. *International Journal of Heat and Mass Transfer*, 1991, **34,** 1149–1161.
18. Circelli, B. R. and McLaughlin, J. B., A numerical study of heat transfer in turbulent shear flow. *Numerical Heat Transfer*, 1986, **9,** 335–348.
19. Brooke, J. W., Transport processes in a direct numerical simulation of turbulent channel flow. Ph.D. thesis, University of Illinois, Urbana, IL, 1994.
20. Kontomaris, K., Hanratty, T. J. and McLaughlin, J. B., An algorithm for tracking fluid particles in a spectral simulation of turbulent channel flow. *Journal of Computational Physics*, 1992, **103,** 231–242.
21. Kontomaris, K. and Hanratty, T. J., Effect of molecular diffusivity on point source diffusion in the center of a numerically simulated turbulent channel flow. *International Journal of Heat and Mass Transfer*, 1994, **37,** 1817–1828.
22. Chandrasekhar, S., Stochastic problems in Physics and Astronomy. *Review of Modern Physics*, 1943, **15,** 1–89.
23. Bird, R. B., Stewart, W. A. and Lightfoot, E. N., *Transport Phenomena*. Wiley, New York, 1960, p. 353.
24. Son, J. B., Limiting relation for the eddy diffusion coefficient close to a wall. M.Sc. thesis, University of Illinois, Urbana, IL, 1965.
25. Van Shaw, P., A study of the fluctuations and the time average of the rate of turbulent mass transfer to a pipe wall. Ph.D. thesis, University of Illinois, Urbana, IL, 1963.
26. Schutz, G., Untersuchung des Stoffaustausch-Anlaufgebietes in einem Rohr bei Vollaus-gebildeter Hydrodynamischer Strömung mit einer Electrochemischen Methode. *International Journal of Heat and Mass Transfer Series*, 1964, **7,** 1077.